LASER INTERFEROMETER GRAVITATIONAL WAVE OBSERVATORY

LIGO Laboratory / LIGO Scientific Collaboration

LIGO-T030023-01-D	*LIGO*	5/12/2003

LIGO Optical Contamination Tests of Hydraulic Fluids

Lee Cardenas, Liyuan Zhang, William Kells and Dennis Coyne

Distribution of this document:
LIGO Science Collaboration

This is an internal working note
of the LIGO Project.

California Institute of Technology
LIGO Project – MS 18-34
1200 E. California Blvd.
Pasadena, CA 91125
Phone (626) 395-2129
Fax (626) 304-9834
E-mail: info@ligo.caltech.edu

Massachusetts Institute of Technology
LIGO Project – NW17-161
175 Albany St
Cambridge, MA 02139
Phone (617) 253-4824
Fax (617) 253-7014
E-mail: info@ligo.mit.edu

LIGO Hanford Observatory
P.O. Box 1970
Mail Stop S9-02
Richland WA 99352
Phone 509-372-8106
Fax 509-372-8137

LIGO Livingston Observatory
P.O. Box 940
Livingston, LA 70754
Phone 225-686-3100
Fax 225-686-7189

http://www.ligo.caltech.edu/

Abstract

This report discusses current contamination experiments and gives a summary on the test results of the hydraulic fluids of HEPI.

1   Introduction

To achieve its goal, LIGO has set a limit on the rate of increase in loss for its optics of no more than 10 ppm/year scatter and 2 ppm/year absorption[1]. Representative samples of each material included in LIGO's vacuum system must be screened experimentally to ensure the material does not induced optical losses exceeding the limit. A contamination experiment based on a high-finesse Fabry-Perot cavity and the rf reflection-locking technique has been developed in LIGO OTF lab[1][2][3]. This report discusses current progress in the contamination experiments and summarizes test results of the hydraulic fluids of HEPI [4].

2   Apparatus and Loss-Measurement Principles

Fig.1 is a schematic diagram of the test bench, it is similar to the Fig.1 of ref.[1] and a detailed description can be found there.
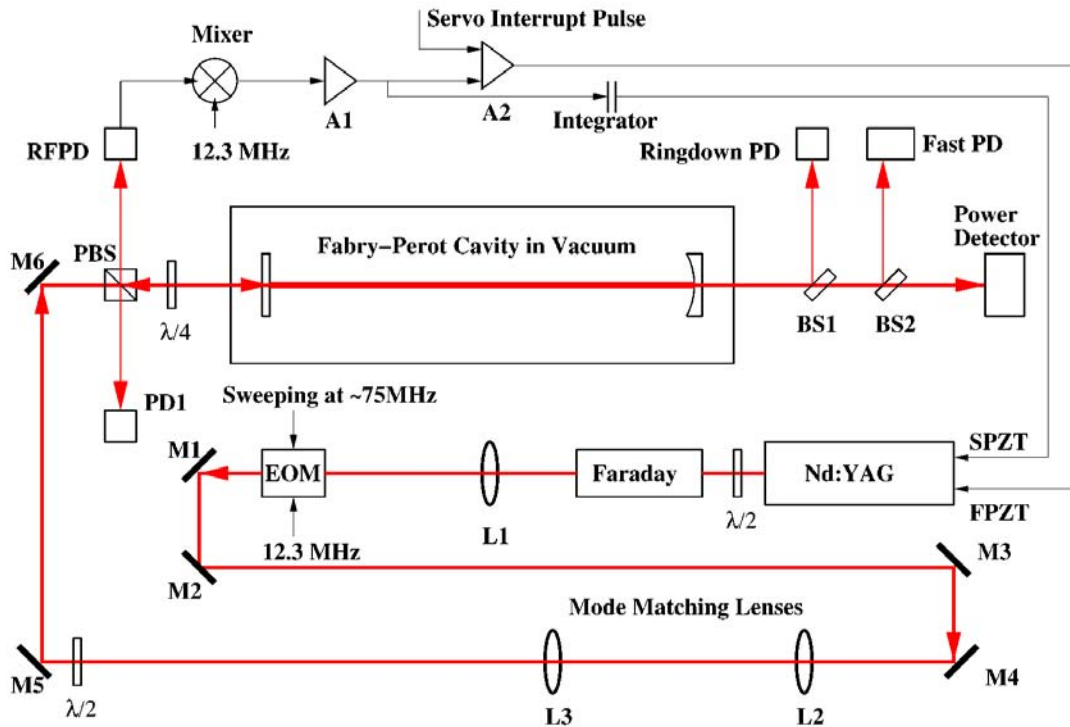

Fig. 1. A schematic diagram of the optical contamination test bench.

The Fabry-Perot cavity is composed of a flat mirror and a concave mirror of 1 m curvature, the transmittance of the two mirrors is ~70 ppm at 1064 nm, and the length of the cavity is 0.5 m. The

laser frequency is locked to one of the cavity resonant TEM_{00} modes, so a steady high power is built in the cavity. By introducing a ~200μs pulse in the second amplifier, the cavity resonance is transitorily disabled and the intracavity power decay can be measured by a photodiode (Ringdown PD) monitoring the transmitted light and a digital scope. The cavity storage time can be got by fitting the cavity power decay using an exponential function, and the cavity total optical loss can be inferred by:

$$L_{loss} = 2l/c\tau, \qquad (1)$$

where l is the cavity length, c the speed of light and τ the cavity power storage time[1].

The surface optical absorption of optics can be inferred from changes of the frequency spacing between the two cavity modes (TEM_{00} and TEM_{01}) caused by thermal expansion of the heated optic surfaces. The frequency spacing between TEM_{00} and TEM_{01} is a function of cavity g factors [1]:

$$\Delta\nu_{00\text{-}01} = c/(2\pi l)\cos^{-1}[g_1 g_2]^{1/2}, \qquad (2)$$

$$g_n = g_{on} + \alpha l I_t A/(2\pi\kappa\omega^2 T), \ n=1,2 \qquad (3)$$

where subscripts 00 and 01 represent the fundamental mode and a first-order mode, subscripts 1 and 2 the two cavity mirrors, g_n is cavity g-factor with surface absorption, g_{on} cavity g-factor with no absorption, A the surface optical absorbance of the heated optic, I_t the cavity transmitted power, ω the beam waist on the optic surface, T output mirror transmissivity, and α and κ are the thermal expansion coefficient and the heat conductivity of the substrate respectively, for fused silica mirrors $\alpha/\kappa = 3.3 \times 10^{-7}$ m/W. In our experiment, the beat frequency $\Delta\nu_{00\text{-}01}$ is around 75 MHz and measured by using a spectrum analyzer, introducing a sweeping rf signal at EOM and monitoring the output beam with a fast photodiode. The beat frequency is usually measured at 8 different power levels with different angles of the half-wave plate before the Faraday isolator, at the same time, the output power is also recorded with a power detector. Finally, by fitting the beat frequency and output power data with above equations (2) and (3), a sum of surface absorbance on the two cavity mirrors can be inferred. Fig. 2. shows a fitting of measurement data, parameter A is the sum of the surface absorbance. If the sample is symmetrically placed around the cavity, we may suppose that the absorbance caused by the surface deposition of gaseous contaminants is roughly equal on the two cavity mirrors.
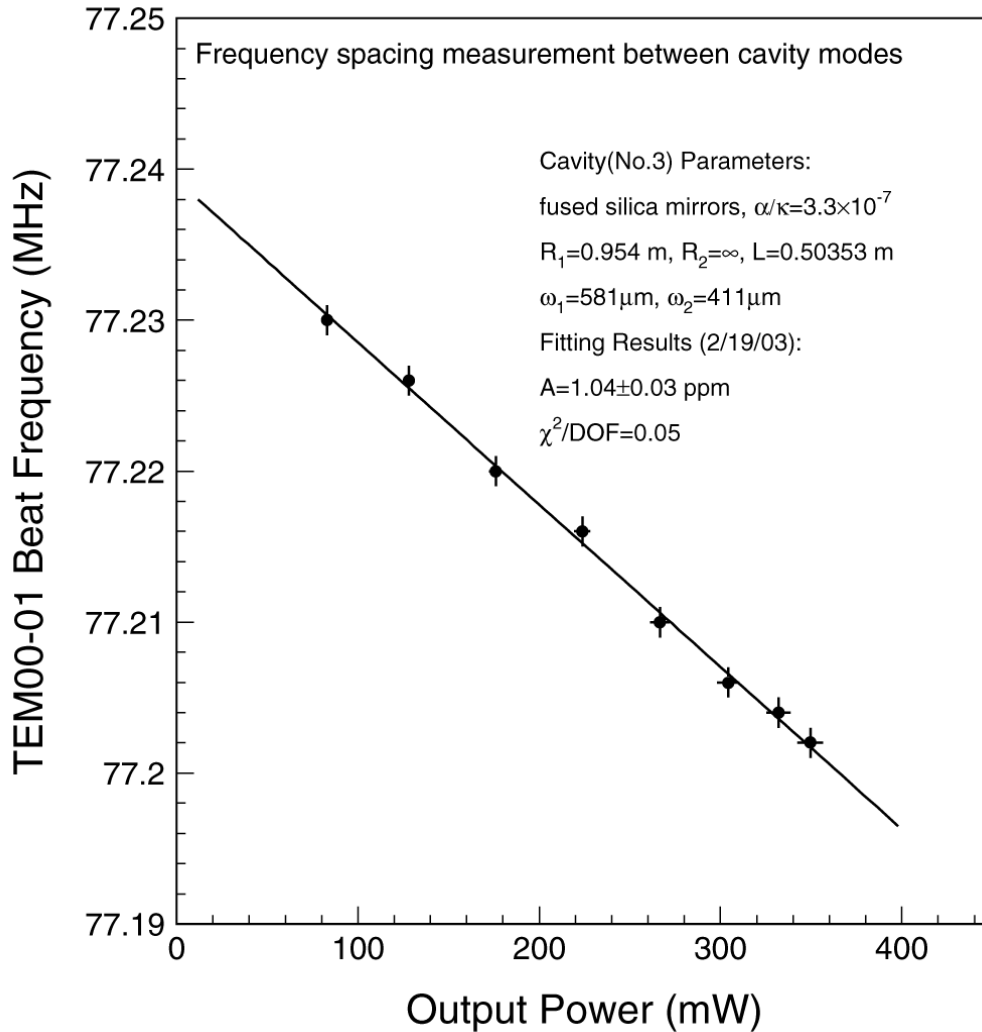
Fig. 2. The frequency spacing between cavity modes as a function of the output power.

3   Sample Description and Preparation

The fluid would not be pressurized when the LIGO vacuum chambers are open or exposed. Nonetheless, there are opportunities for contaminants to migrate into the vacuum system. Two possible scenarios are as follows:

a) A spill or leak occurs outside the vacuum system but near a chamber. Either the leak is undetected (because it is quite small) or it is cleaned up, but some residual fluid exists. Later an entry is made into the system and the fluid migrates into the chamber through glove or booty contact with some residual fluid.

b) During a vacuum system entry, a non-pressurized, but wetted fluid line is overstressed in an accident (e.g. caught on a crane or forklift). While it is likely positive measures or blocks can be designed into the system to prevent these scenarios, it is conceivable that an unanticipated failure might occur, however small the probability might be. The fluid would, of course, be

cleaned up with water (most are water soluble) and light, aromatic solvents (ethyl alcohol, methanol, isopropanol). Nonetheless a residual film of the contaminant would remain.

The hydraulic fluid samples were introduced to the cavity by placing two single contaminated stainless steel bars (each 2" wide by 3/16" thick by 12" long) into the chamber. The bars were first cleaned and vacuum baked to ensure that there were no contaminants. The bars were then completely wetted with the sample fluid (with LIGO approved nitrile or nylon gloved hands). The fluid was then wiped off of the bar with a LIGO approved clean-room cloth/wipe until it it no longer appeared to be wet with the fluid. This was an attempt to simulate the amount of surface contamination that one might have in a scenario in which a leak occurs near a LIGO chamber. The spacer between the two cavity mirrors (a fused silica tube) prevents direct free molecular streaming to the cavity mirrors by the contaminant. There are holes in this spacer so that diffusion from the contaminated sample into the cavity space does occur.

The potential hydraulic fluids for the Hydraulic External Pre-Isolator (HEPI) system [4], which were tested are as follows:

a) Mineral Oil. Mineral oil is the fluid used in all quiet hydraulic applications to date. The disadvantage with mineral oil is that it is not water soluble and harder to clean up.

b) Glycerin. Glycerin is water soluble and non-flamable but too viscous by itself. Water based additives to prevent biological growth and inhibit rust may also act as optical contaminants.

c) Glycerin (65%) and Ethyl Alcohol (35%). An ethyl alcohol and glycerin mixture has the correct viscosity, does not support biological growth, does not cause corrosion and may have adequate lubroscity. However the mixture is flamable.

d) Aquamil. Aquamil is a fire resistant hydraulic fluid that provides excellent performance in hydraulically operated food processing equipment. It is a high performance water glycol fire resistant hydraulic fluid and specially formulated for use in food plant applications.

e) Chemsol. Chemsol SPFRHF is a new generation, high-performance water-glycol hydraulic fluid designed to operate at pressures up to 7000 psi (483 bars). Synonyms SPFRHF stands for Supreme Performance Fire Retardant Hydraulic Fluid.

f) Chem Draw # HSF-75-2. Chem.-Draw HSF-75-2 is a water dilutable synthetic lubricant formulated to meet the demands of the internal water hydraulic systems of high-pressure hydro forming presses. It is also formulated to serve as an internal and external lubricant for low-pressure and pressure-sequence hydro forming applications.

4   Results and Discussion

Fig.3, 4, 5, 6 and 7 are the results of the cavity 1 without sample (reference running) and with samples. Fig.8 is the result of our first test with cavity 2 and mineral oil sample. Fig.9, 10 and 11 are the results of cavity 3 without sample, with a Chem-Draw and an Undyed Chem-Sol respectively. In the first test, the systematic error was too big, as shown in Fig.8, especially in the Ringdown measurement. After the experiment, one of the chamber clamps was found to be broken, probably it's the reason.   Like in previous work[2] some tests showed a big decrease in total loss for the starting period, this could be due to that the mirror coating absorbed water or some other contamination before evacuation, which is then desorbed in

vacuum. Whatever the explanation, the conservative estimate could be obtained by starting the linear fit after the initial downward trend. Table 1 is a summary of the above test results, except for the Mineral Oil, all other samples meet the LIGO requirements. Although we do not expect each test to have the same background, a more conservative estimation for each sample tested in cavities 1 and 3 could be obtained by subtracting the reference running result of the corresponding empty cavity. If one subtracts the reference loss, then the results are still within the LIGO requirements.

Table 1. Annual loss predictions of the tested hydraulic fluids.

Sample	Cavity No.	Absorption Loss (ppm/year)	Total Loss (ppm/year)
No sample	1	-0.2 ± 0.7	-5 ± 2
Glycerin	1	-0.2 ± 0.8	-0.5 ± 2
Glycerin (65%) +Ethyl (35%)	1	-0.8 ± 0.7	-12 ± 3
Aquamill	1	0.2 ± 0.4	-8 ± 2
Chem-Sol	1	-0.3 ± 0.3	-6.6 ± 2
Mineral Oil	2	3 ± 0.7	13 ± 2
No sample	3	0.5 ± 0.5	-1 ± 3
Chem Draw #HSF-75-2	3	0.1 ± 0.6	-1 ± 2
Undyed Chem-Sol	3	0.0 ± 0.4	-2 ± 2
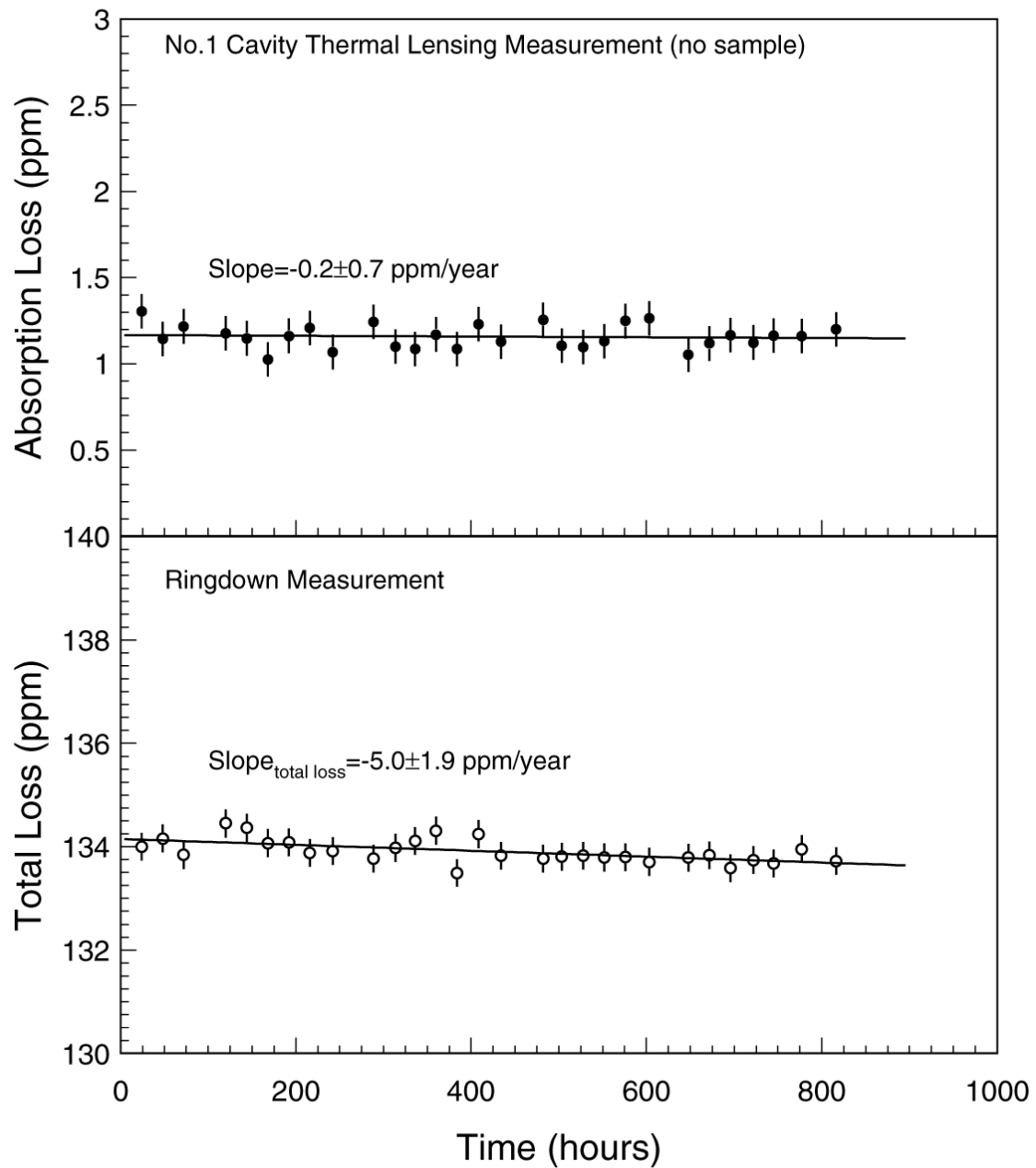
Fig.3   The mirror surface absorption and the total loss versus time of the cavity 1 without sample.
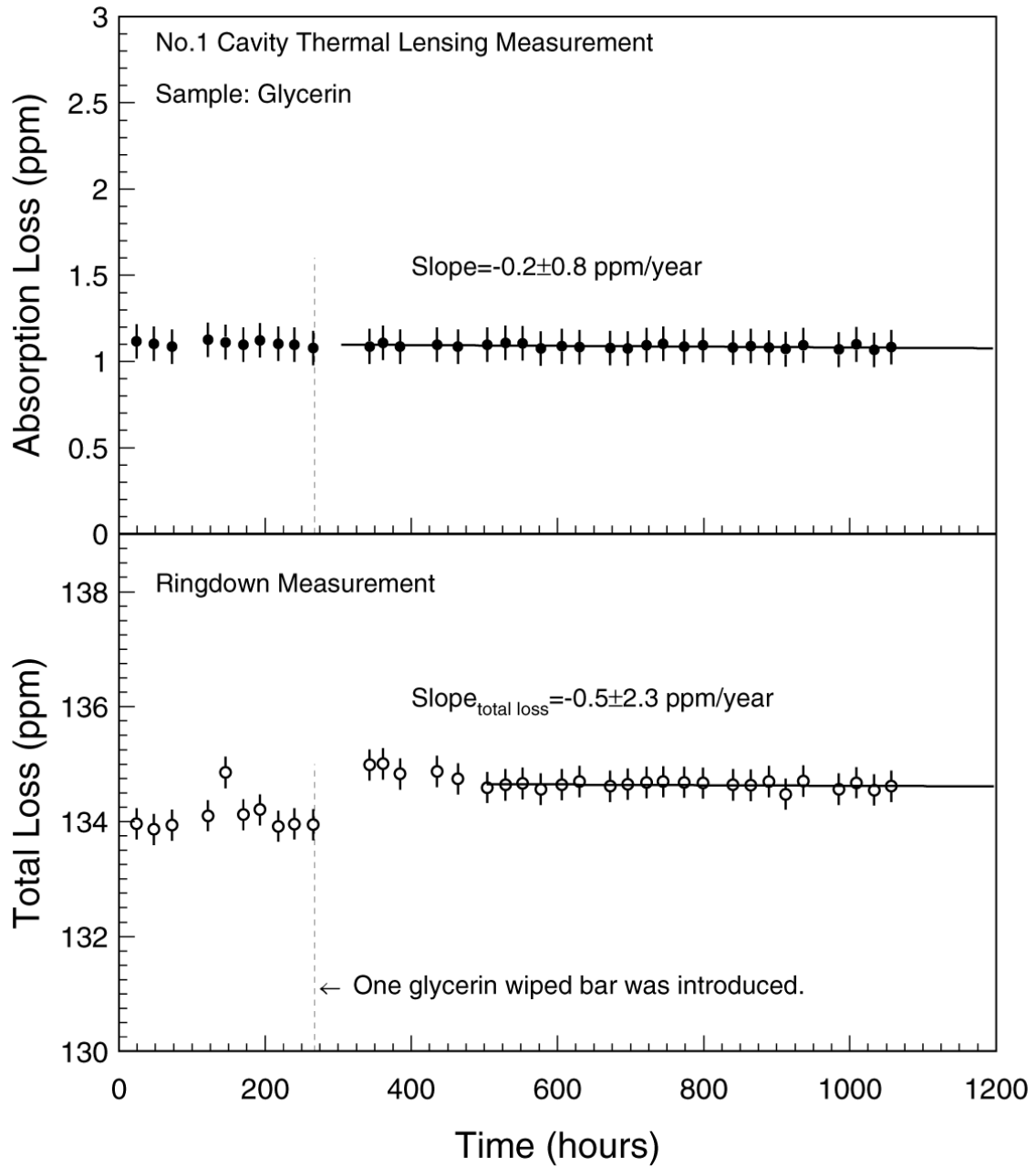
Fig.4   The mirror surface absorption and the total loss versus time of the cavity 1 with the sample of Glycerin.
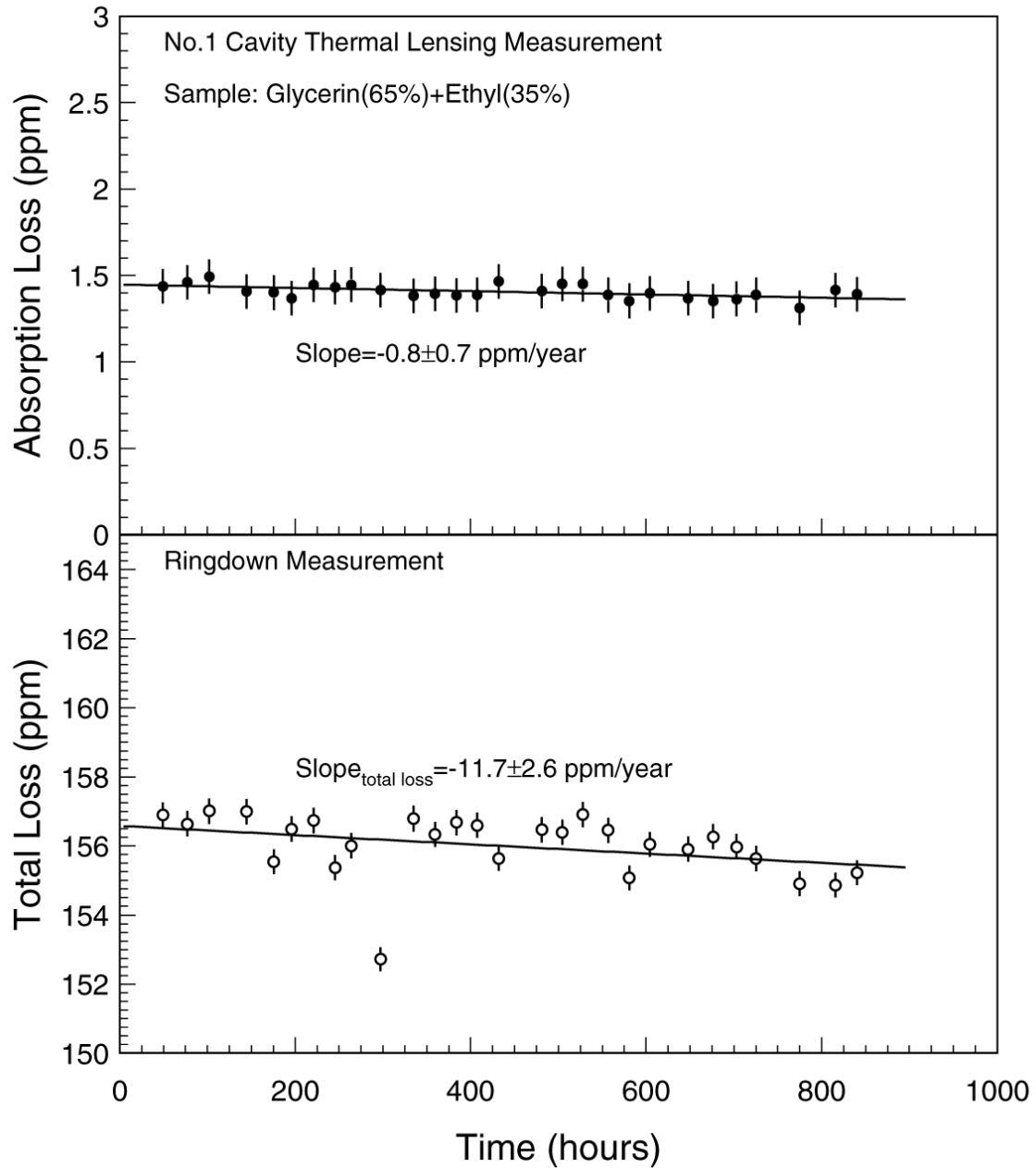
Fig.5   The mirror surface absorption and the total loss versus time of the cavity 1 with the sample of Glycerin (65%) + Ethyl (35%).
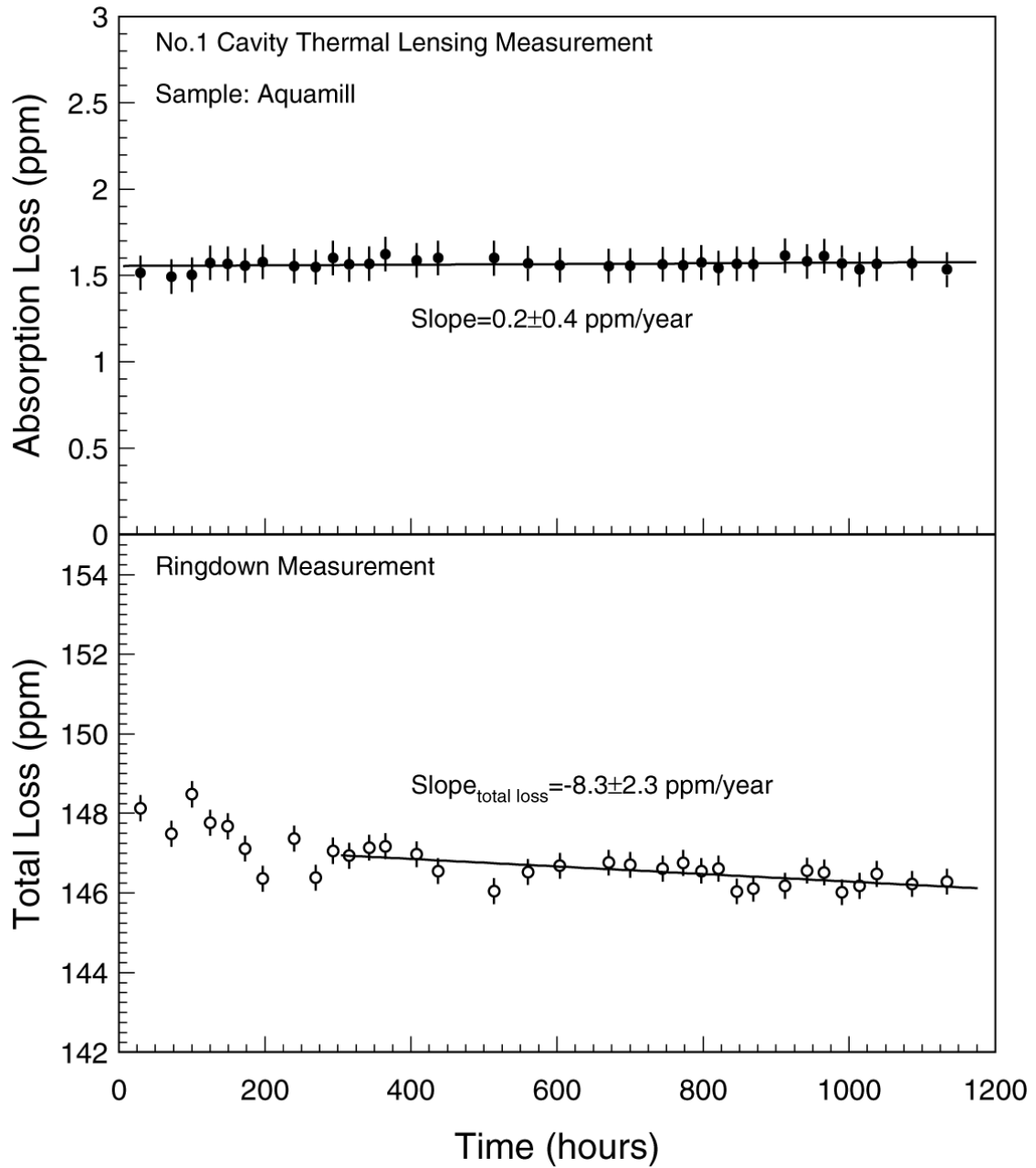
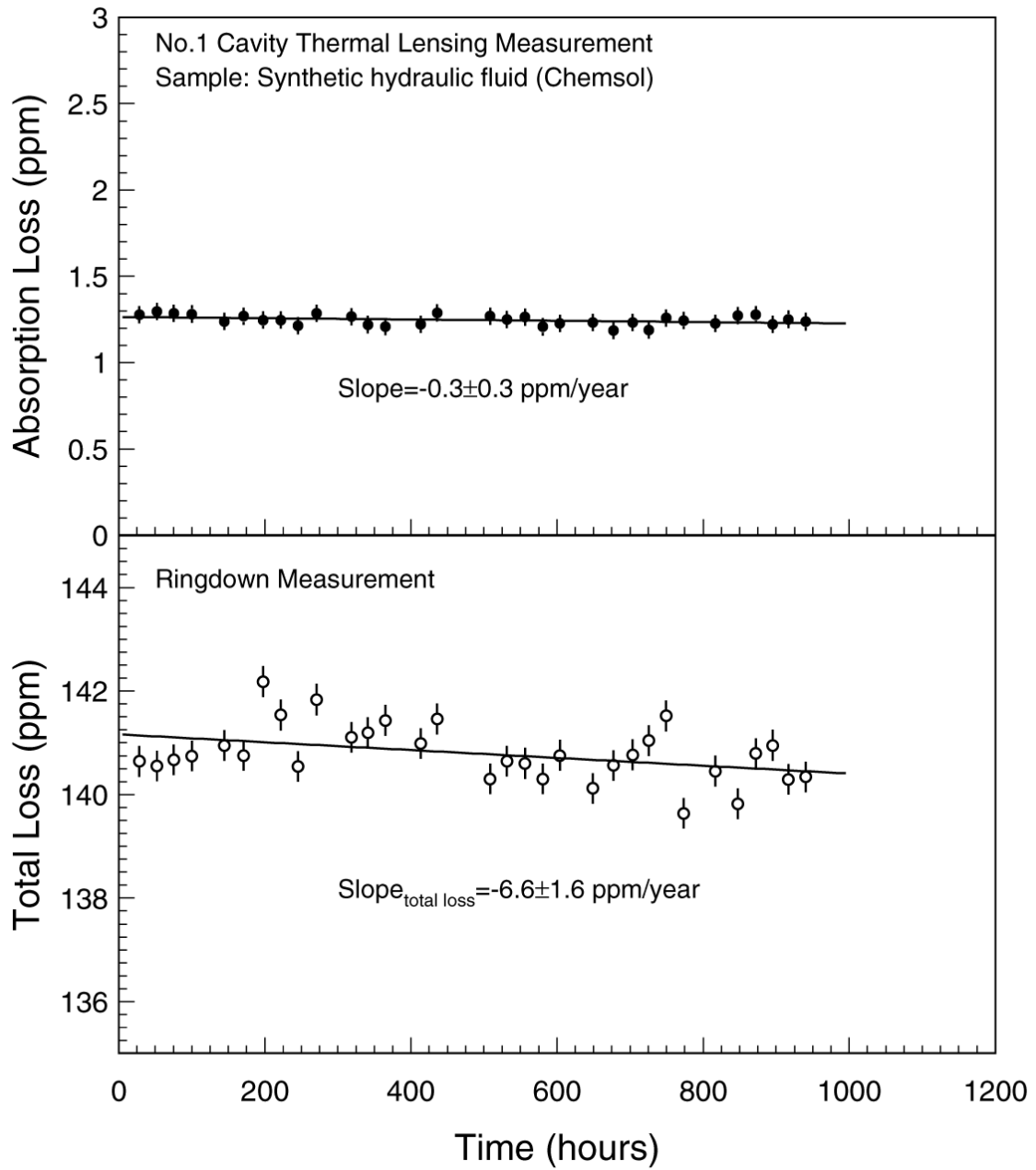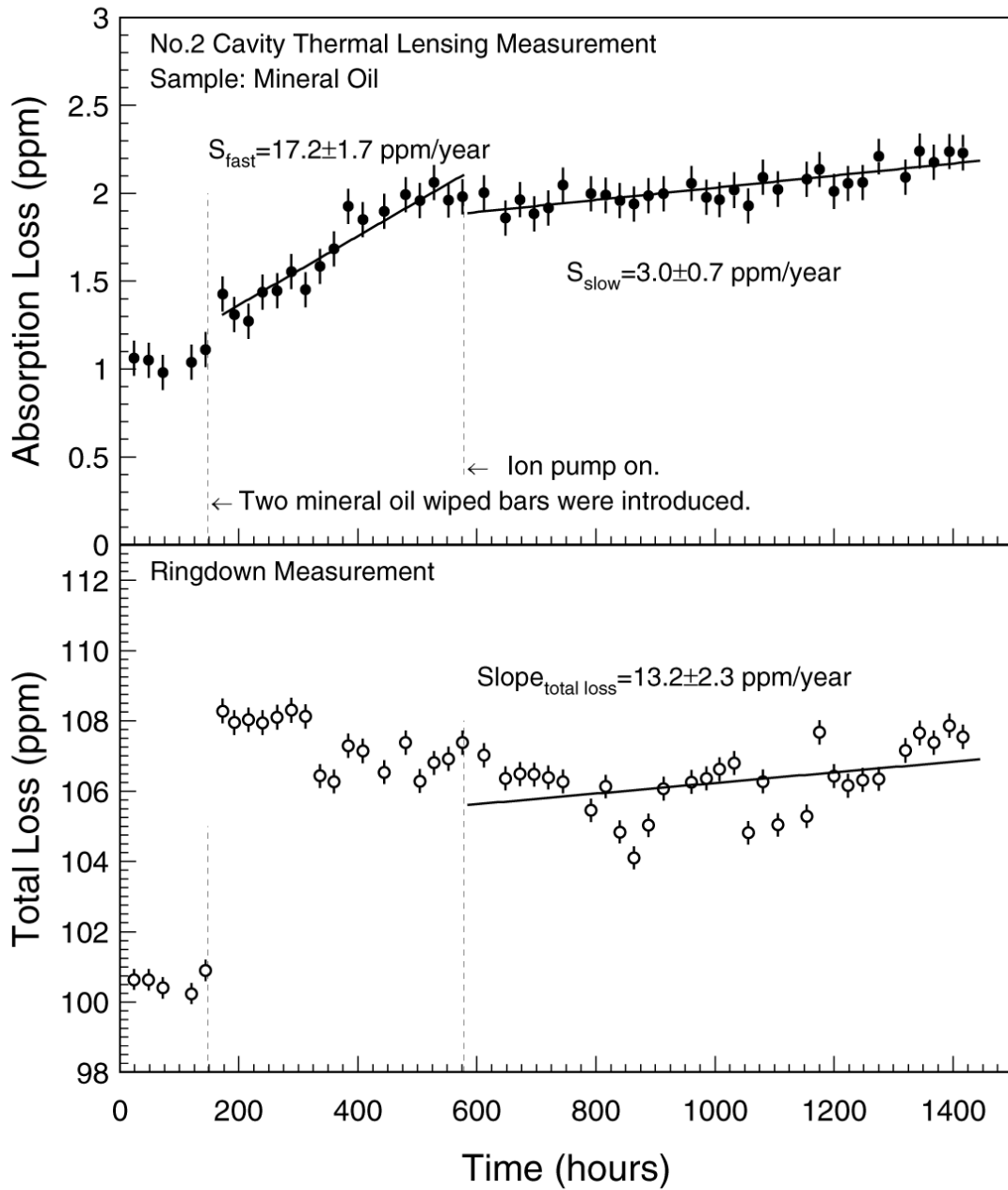Fig.6   The mirror surface absorption and the total loss versus time of the cavity 1 with the sample of Aquamill.

Fig.7 The mirror surface absorption and the total loss versus time of the cavity 1 with the sample of Chemsol.

Fig.8   The mirror surface absorption and the total loss versus time of the cavity 2 with the sample of Mineral Oil.
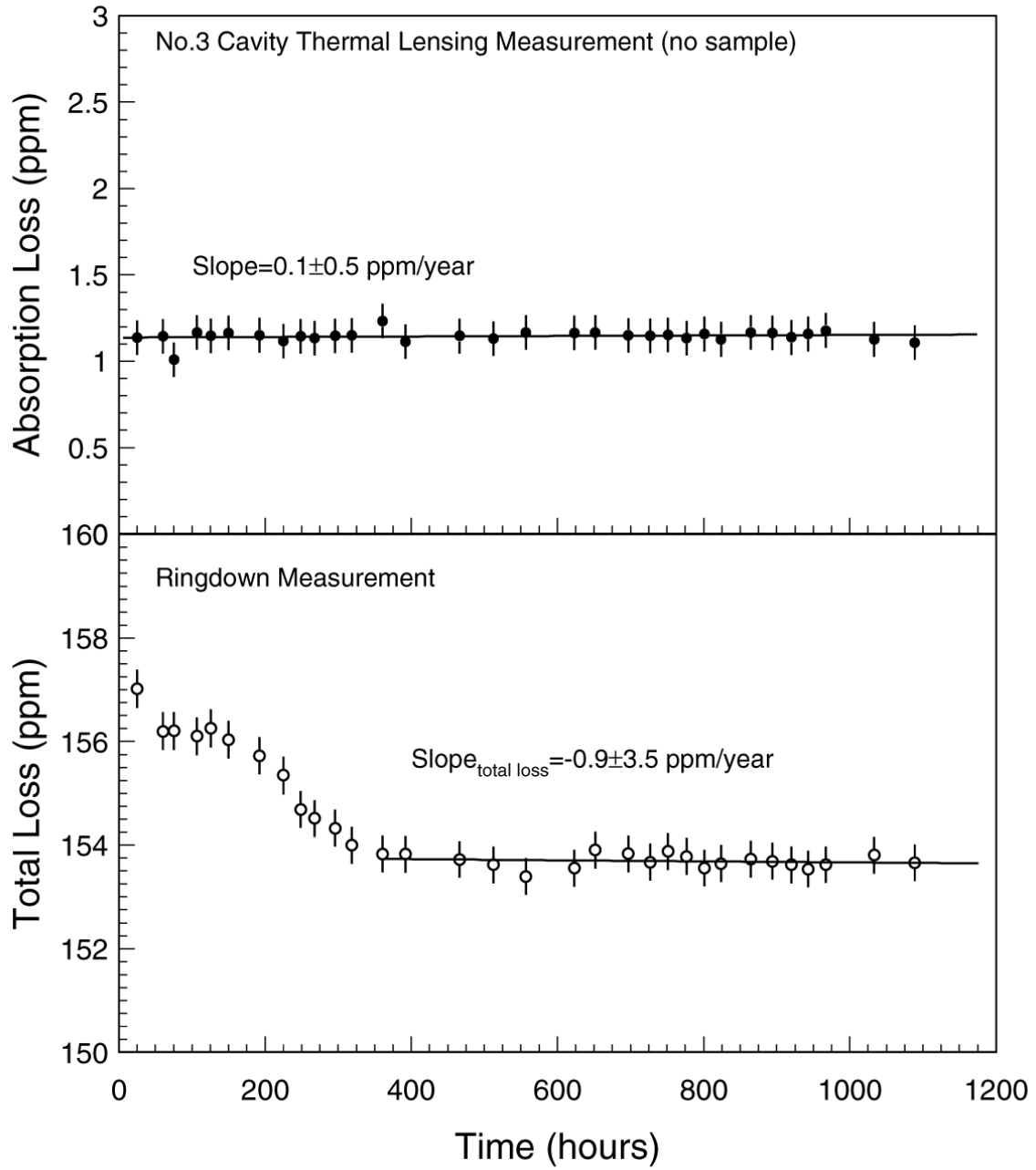
Fig.9 The mirror surface absorption and the total loss versus time of the cavity 3 without sample.
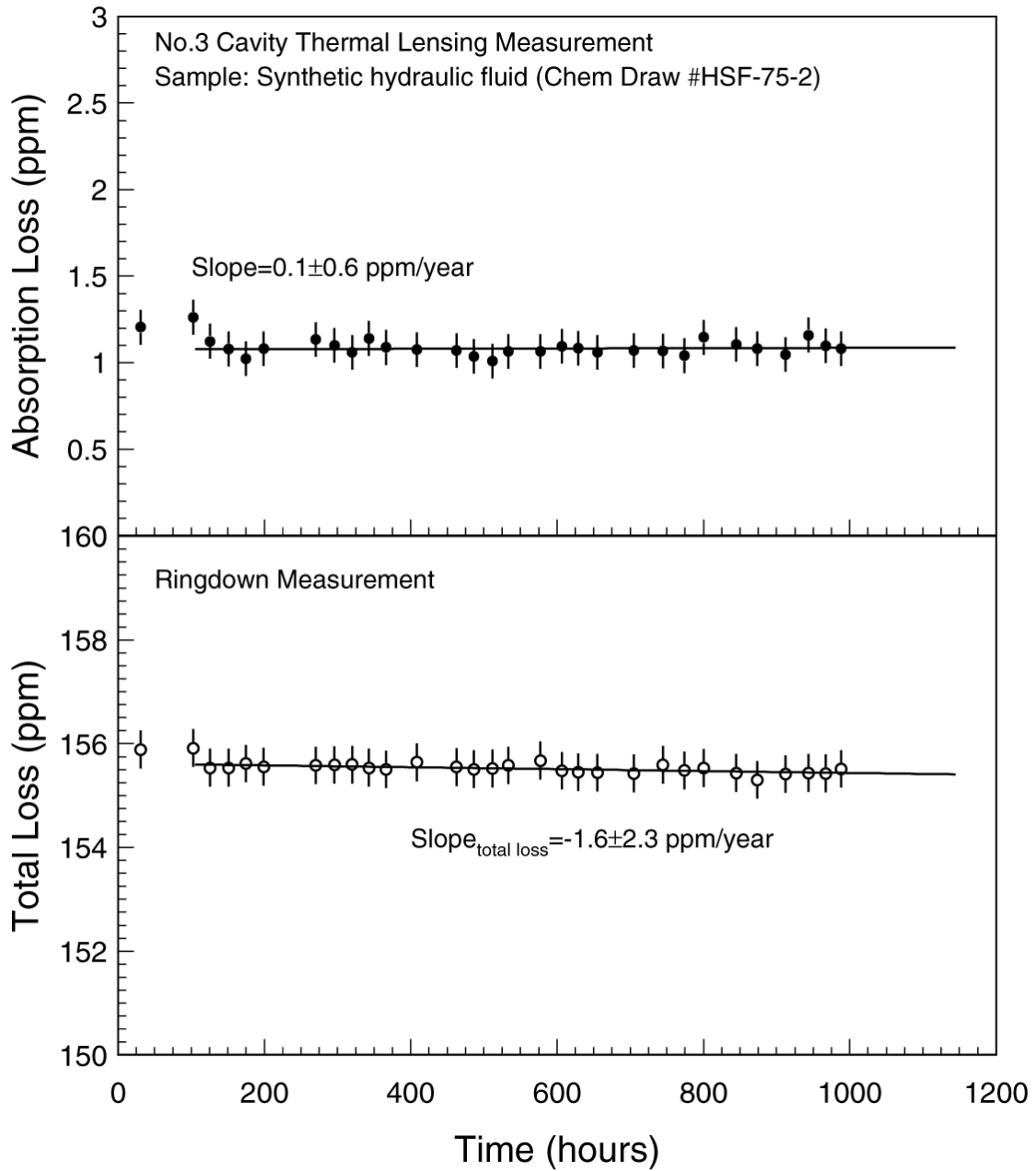
Fig.10 The mirror surface absorption and the total loss versus time of the cavity 3 with the sample of Chem Draw #HSF-75-2.
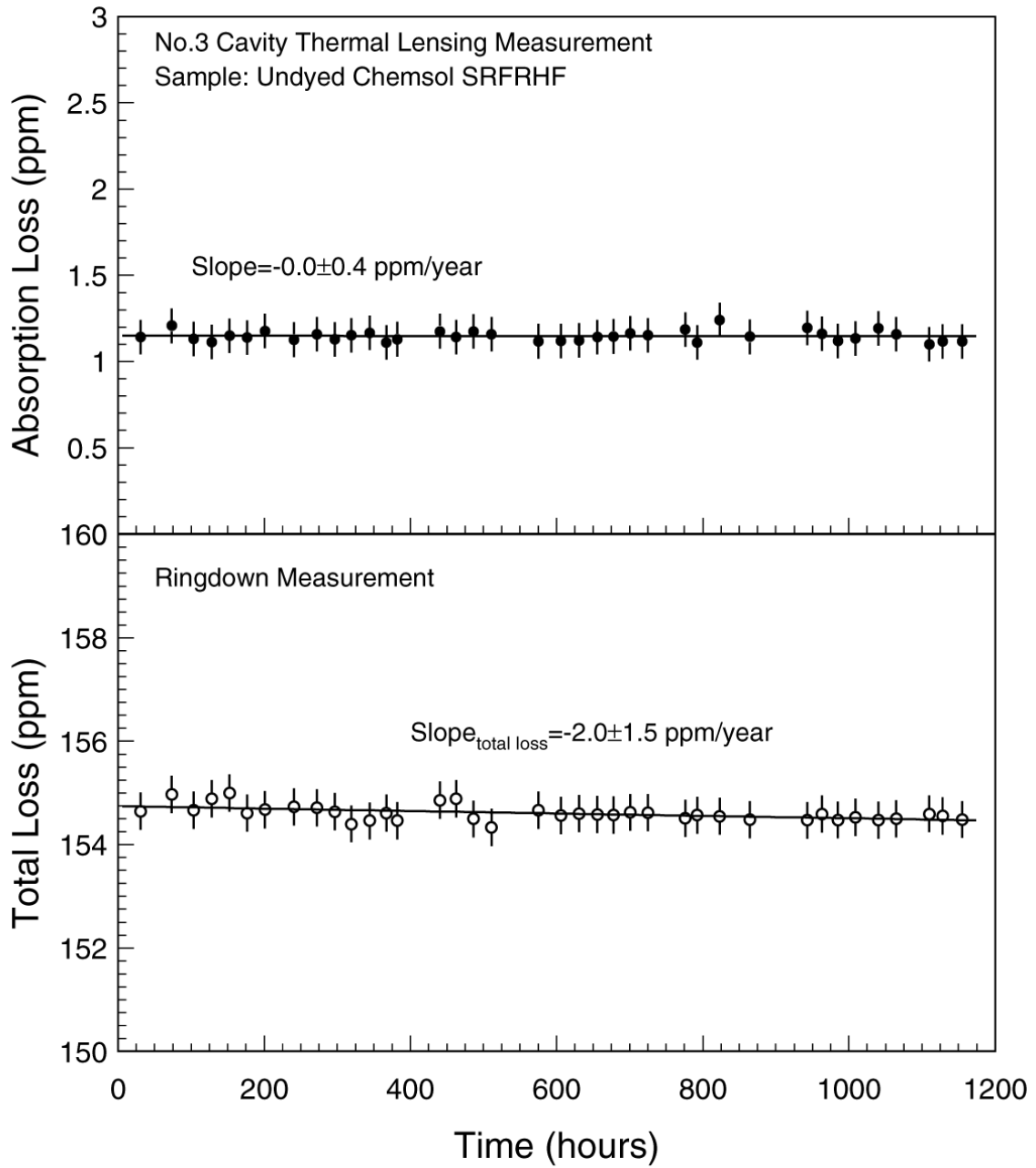
Fig.11   The mirror surface absorption and the total loss versus time of the cavity 3 with the sample of Undyed Chem-Sol (SRFRHF).

Acknowledgments

References

1. Daqun Li, Dennis Coyne, and Jordan Camp, "Optical contamination screening of materials with a high-finesse Fabry-Perot cavity resonated continuously at 1.06-µm wavelength in vacuum", Appl. Opt. **38**, 5378-5383 (1999).

2. A. Abramovici, T. T. Lyons, and F. J. Raab, "Measured limits to contamination of optical surface by elastomers in vacuum", Appl. Opt. **34**, 183-185 (1995).

3. Daqun Li and Jordan Camp, "Current Progress in LIGO Optical Contamination Studies", **LIGO-T980003-00-D**.

4. Rich Abbott, et. al., **LIGO-G030196-00**.